



Published in final edited form as:

J Orthop Res. 2008 October ; 26(10): 1384–1389. doi:10.1002/jor.20667.

Effect of age on vascularization during fracture repair

Chuangyong Lu, Erik Hansen, Anna Sapozhnikova, Diane Hu, Theodore Miclau, and Ralph S. Marcucio⁺

Department of Orthopaedic Surgery, University of California at San Francisco, San Francisco, CA.

Abstract

Age affects fracture repair, however the underlying mechanisms are not well understood. The goal of this study was to assess the effects that age has on vascularization during fracture healing. Tibial fractures were created in juvenile (4-week-old), middle-aged (6-month-old), and elderly (18-month-old) mice. The length density and surface density of blood vessels within fracture calluses were analyzed using stereology at 7 days after fracture. The expression of molecules that regulate vascular invasion of the fracture callus was also compared among the three age groups by immunohistochemistry and *in situ* hybridization. At 7 days after fracture, juvenile mice had a higher surface density of blood vessels compared to the middle-aged and elderly. Hypoxia-inducible factor-1 α protein and transcripts of *vascular endothelial growth factor* were detected at 3 days post-injury in juvenile but not middle-aged and elderly mice. Stronger *Mmp-9* and *-13* expression was detected in fracture calluses at day 7 in the juvenile compared to the middle-aged and elderly mice. At 21 days post-fracture, expression of both *Mmps* was more robust in the elderly than juvenile and middle-aged animals. These data indicate that age affects vascularization during fracture repair, and the changes we observed are directly correlated with altered expression of biochemical factors that regulate the process of angiogenesis. However, whether the increased vascularization is the cause or result of accelerated bone repair in juvenile animals remains unknown. Nonetheless, our results indicate that enhancing vascularization during fracture repair in the elderly may provide unique therapeutic opportunities.

Keywords

fracture; age; aging; angiogenesis; vascularization

Introduction

There are age-related changes in bone repair. Juveniles heal much more rapidly than adults^{1, 2}, but the effect of age on fracture healing in adults remains controversial^{3, 4}. Our previous study in mice⁵ has demonstrated that 4-week juvenile mice heal fractures more quickly than 6-month adults, and that healing capacity continues to decline as animals grow beyond middle-age. Multiple factors could contribute to the age-related changes in fracture healing, such as decreased number and/or function of stem cells^{6, 7}, structural and cellular changes in periosteum⁸, decreased chondrogenic potential of periosteum⁹, and changes in the local signaling milieu at fracture site^{10, 11}. However, the effect of age on vascularization during fracture healing has not been well determined. Our objective was to determine the extent to which increased vascularization could underlie the rapid healing response in juvenile animals, and assess whether changes in the vascular response during fracture repair occurred throughout the lifespan of an animal.

⁺Author for correspondence: Phone: 415-206-5366, Fax: 415-206-8244, Ralph.Marcucio@ucsf.edu.

Tissue vascularization is essential for successful bone healing 12, 13. Two mechanisms, angiogenesis and vasculogenesis, could contribute to the vascularization of a fracture callus. Angiogenesis is sprouting of new capillary vessels from existing vessels. Vasculogenesis refers to the formation of new blood vessels via aggregation and condensation of circulating endothelial progenitor cells into vascular cords 14. Vascularization is a complex process that involves coordination among multiple pro- and anti-angiogenic factors. For example, aerobic production of lactate stimulates angiogenesis by stabilizing Hypoxia-Inducible Factor 1-alpha (Hif-1 α) at the injury site 15, 16. This molecule, in combination with Hif-1 β , then forms a hypoxia-dependent transcription factor complex that up-regulates the expression of hypoxia-inducible genes, including Vascular Endothelial Growth Factor (VEGF) 17. VEGF mediates angiogenesis by stimulating proliferation of endothelial cells and promoting vascular invasion into a variety of tissues 18. Invasion of tissues by endothelial cells, and degradation of the cartilage matrix during endochondral ossification by endothelial cells requires the activities of matrix metalloproteinases (MMPs). MMP-9 19, 20 and MMP-13 21, 22, mediate part of this process during fracture repair and skeletal development.

There is accumulating evidence suggesting that age affects both angiogenesis and vasculogenesis 23–25. For example, Klotho mutant mice, a rodent model of aging, exhibit impaired microvascular sprouting from cultured aortic rings and have a lower rate of incorporation of transplanted bone marrow cells into capillaries in ischemic tissues, compared to wild type controls 25. The goal of our current work was to examine the effect that age has on vascularization during fracture repair. In this study, vascularization of fracture calluses and the expression of molecules that regulate vascular invasion of the fracture callus (Hif-1 α , VEGF, MMP9 and 13) were compared among juvenile, middle-aged, and elderly mice during repair of a tibial fracture.

Materials and Methods

Creation of tibial fractures

All procedures were approved by the IACUC at University of California at San Francisco. Male mice (129J/B6) were used in this study. Juvenile (4 weeks), middle-aged (6 months), and elderly (18 months) mice were anesthetized by intra-peritoneal injection of 2% Avertin (0.015ml/g). A transverse fracture at the mid-shaft of the right tibia was generated by three-point bending and was left unstabilized 5. Mice were allowed to move freely after recovering from anesthesia. Analgesic (Buprenex, 0.05–0.1 mg/kg) was administered immediately after surgery.

Tissue processing and histologic staining

Animals (n=5/time point/age group) were sacrificed at 3, 5, 7, 10, 14, and 21 days post-fracture. To ensure adequate preservation of the soft callus the fractured tibiae were collected with the surrounding muscles intact and immediately placed into 4% paraformaldehyde. The tissues were decalcified in 19% EDTA, dehydrated, and embedded in wax. Longitudinal sections (10 μ m, sagittal) were prepared through the whole callus. To visualize cartilage and bone in fracture calluses, every tenth slide was stained with Safranin O and Fast Green 5.

PECAM immunohistochemistry and quantification of the vasculature in fracture calluses

To compare vascularization in the fractured limbs among the different age groups, immunohistochemistry using an anti-PECAM (platelet endothelial cell adhesion molecule) antibody was performed to visualize blood vessels 5, 26. Briefly, a slide obtained from near the middle of the fracture callus from each sample of 7 days after fracture (n=4–5/age group) was dewaxed and rehydrated. The tissues were first incubated with an anti-PECAM-1 antibody (PharMingen, San Diego, CA. 1:50) overnight at 4°C, then with a second antibody (biotinylated

goat anti-rat IgG, Pharmingen, San Diego, CA.), and finally with streptavidin-horseradish peroxidase (Amersham, Piscataway, NJ). The immune complexes were visualized using diaminobenzidine (DAB) as the substrate, and the tissues were counterstained with methyl green.

The length and the area of the outer surface of blood vessels within calluses were estimated by analyzing the length density (the length of blood vessels per unit volume of the reference space, L_v) and surface density (the area of the outer surface of blood vessels per unit volume of the reference space, S_v) 27, 28 using an Olympus CAST system (Olympus, Center Valley, PA) and software by Visiopharm (Visiopharm, Hørsholm, Denmark). The fracture callus was outlined using low magnification (40 \times). The length density was estimated using high magnification (200 \times) and a count frame probe. Forty to fifty fields that covered approximately 50% of the fracture callus were systematically acquired using unbiased uniform random sampling. Four counting frames that covered 50% of the area within a field were overlain on each field. The number of blood vessels (q) within the fracture callus was counted within each frame. The area of the callus that was analyzed was determined by counting the number of points (p) within the counting frame that fell on callus tissue. This configuration was pre-determined to achieve approximately 200 counts for blood vessel profiles on each section, because this is optimal for deriving accurate and precise estimates using stereology 28. In this configuration, the area per point (a/p) is 5915.6 mm². Length density was calculated as: $L_v = 2 * \Sigma(q) / (\Sigma(p) * a/p)$.

Similarly, the surface density of the blood vessels within fracture callus was determined using high magnification (200 \times). Ten to twenty high magnification fields that covered approximately 10% of the callus area were systematically acquired using uniform random sampling. Randomly oriented line probes with points were then applied to each field. The points that fell onto callus tissue (p) and the number of intersections (i) between the outer surface of blood vessels and the line probes were quantified. The surface density was calculated as: $S_v = 2 * \Sigma(i) / ((l/p) * \Sigma(p))$. Using this configuration, the length per point (l/p) is 22.25 μ m.

It has been shown before that at 7 days after fracture juvenile mice have more cartilage in fracture callus than middle-aged and elderly mice⁵. Because cartilage is avascular, different proportions of cartilage in fracture callus will affect the estimation of L_v and S_v . To eliminate the impact of cartilage, L_v and S_v were adjusted to account for the percentage of cartilage in the callus. Briefly, area of the callus (A_{callus}) and cartilage (A_{cart}) was analyzed on Safranin O/Fast Green stained sections that were adjacent to those used for PECAM immunostaining. Micrographs of the sections were acquired using a Leica microscope and Adobe Photoshop. A_{callus} was determined by outlining the callus and A_{cart} was determined by selection of cartilage. The ratio of cartilage to callus was calculated as A_{cart}/A_{callus} . Adjusted L_v and S_v , L_v^* and S_v^* respectively, were calculated as $L_v^* = L_v / (1 - A_{cart}/A_{callus})$ and $S_v^* = S_v / (1 - A_{cart}/A_{callus})$.

Hif-1 α immunohistochemistry

Immunostaining was performed to detect the stabilization of Hif-1 α in the fracture callus ($n=2-4$ /time point/age group, days 3, 5, and 7). Paraffin sections were dewaxed, rehydrated, and quenched using 0.3% H₂O₂ in methanol. Tissues were incubated with a goat anti-mouse HIF-1 α polyclonal antibody (Santa Cruz Biotechnology, Santa Cruz, CA. 1:200 in PBS) at 4 $^{\circ}$ C overnight. A peroxidase-conjugated affinity purified rabbit anti-goat IgG (H+L) (Jackson Laboratories, Bar Harbor, ME. 1:500 in PBS) was then applied to detect the primary antibody. The antigen-antibody complex was visualized with the DAB reaction.

In situ hybridization

To detect transcripts encoding *VEGF*, *Mmp9*, and *Mmp13*, *in situ* hybridization was performed as described⁵ on the sections adjacent to those used for PECAM immunostaining (n=2–5/time point/age group). Briefly, subclones of cDNA corresponding to the murine *VEGF*, *Mmp9*, and *Mmp13* genes were used to generate ³⁵S-UTP-labelled riboprobes. Prepared sections were hybridized with probes, washed with increasing stringency, coated with emulsion, and exposed for 7–14 days. Hoechst dye was used to stain the nuclei, and a pseudo-colored image of the exposed silver grains was superimposed on the fluorescent image of the nuclei in Adobe Photoshop CS. The location and intensity of the expression of *VEGF*, *Mmp9*, and *Mmp13* transcripts were assessed by three independent observers and representative micrographs are presented.

Statistical analysis

Single factor ANOVA and t-test were used to determine the effect of age on Lv, Lv*, Sv, and Sv*. Data are presented as mean ± one standard deviation.

Results

Lower surface density of vasculature in middle-aged and elderly mice

In this work we examined the length and the area of outer surface of blood vessels within the fracture callus. At 7 days after fracture, cartilage and bone were observed in fracture calluses of all three age groups. Juvenile mice exhibited more cartilage than the middle-aged and elderly (Fig. 1A, D, G). PECAM positive blood vessels were detected throughout the calluses of all three age groups (Fig. 1B, E, H). Blood vessels within the calluses of middle-aged and elderly mice appeared smaller than those observed in the juveniles (Fig. 1C, F, I).

Further histomorphometric analyses demonstrated that mice from all three age groups formed a similar amount of callus tissue at day 7. The area of cartilage (Acart) and the percentage of cartilage to callus (Acart/Acallus) in juvenile mice were significantly higher than in the middle-aged and elderly mice (Fig. 2A). No significant difference was found in the absolute (Lv) and adjusted (Lv*) length density of the blood vessels among three age groups (Fig. 2B). However, the surface density of the blood vessels (Sv) was significantly higher in the juvenile than elderly mice (Fig. 2C, p<0.05). When the percentage of cartilage in callus was considered, the juvenile exhibited significantly higher Sv* than both the middle-aged (p<0.01) and elderly (p<0.01, Fig. 2C). No significant difference was detected in the Sv or Sv* between the middle-aged and elderly (p=0.66).

Age affects expression of Hif-1 α and VEGF in fracture calluses

To begin to elucidate the mechanisms that underlie the differences in vascularization in these groups of mice, we examined the expression profile of two important regulators of angiogenesis. The spatial distribution patterns of HIF-1 α protein and *VEGF* transcripts were visualized by immunohistochemistry and *in situ* hybridization respectively at 3, 5, and 7 days after fracture.

HIF-1 α exhibited differential expression in the three age groups. At day 3, HIF-1 α protein was detected in some chondrocytes located within the reactive periosteum in juvenile mice (Fig. 3A). At this time, the periosteal reaction was not as robust in the adult mice as in the juvenile, and HIF-1 α was not detected in the fracture calluses of middle-aged and elderly mice (Fig. 3B, C). At day 5, HIF-1 α protein was detected in chondrocytes that were in the fracture calluses in all three age groups (Fig. 3D, E, F). By 7 days, robust HIF-1 α expression was observed in chondrocytes in all three age groups (Fig. 3G, H, I).

Similarly, *VEGF* exhibited an early onset of expression in the juvenile mice. At 3 days post-fracture, *VEGF* transcripts were detected in chondrocytes in the reactive periosteum of juvenile mice (Fig. 4A), but not the middle-aged and elderly (Fig. 4B, C). At 5 days after fracture, *VEGF* was observed in chondrocytes in all three age groups, and its expression was more robust in the juvenile (Fig. 4D) compared to the middle-aged and elderly mice (Fig. 4E, F). At day 7, robust *VEGF* expression was observed in fracture calluses of all three ages, but it remained stronger in the juvenile (Fig. 4G) than in the adults (Fig. 4H, I).

Altered expression of MMP-9 and -13 in adult mice

MMP-9¹⁹ and MMP-13²¹ are both required for degradation of the cartilage matrix and vascular invasion during endochondral ossification. Expression of *Mmp-9* (Fig. 5) and *-13* (Fig. 6) transcripts were assessed at 7, 10, 14, and 21 days post-fracture by *in situ* hybridization. These time points were chosen because in our murine model endochondral ossification occurs during this time frame⁵. *Mmp-9* and *-13* exhibited similar patterns of expression. At 7 days after fracture, *Mmp-9* (Fig. 5A) and *-13* (Fig. 6A) transcripts were expressed at high levels at the endochondral front of juvenile mice. At this time point, weak *Mmp-9* and *-13* expression was detected in middle-aged (Fig 5B· Fig 6B) and elderly mice (Fig 5C· Fig 6C). At days 10 and 14, endochondral ossification was robust and *Mmp-9* and *-13* were expressed in mice comprising each age group (Fig 5D–I· Fig 6D–I). At 21 days post-fracture, cartilage has been largely replaced by bone in the juvenile and middle-aged mice (Fig 5 and Fig 6, and see 5) and *Mmp-9* and *-13* expression was limited to the edge of callus (Fig 5J, K and Fig 6J, K). In contrast, cartilage is still present in elderly mice at this stage (Fig 5 and Fig 6, and see 5) and the expression of both *Mmp-9* and *-13* was still robust within the callus (Fig 5L, Fig 6L).

Discussion

Age affects vascularization during fracture healing

In this work, we detected that various components of vascularization during fracture repair are affected by age. In addition to the increased surface density of blood vessels in juvenile animals, age also alters the expression patterns of HIF-1 α protein and *VEGF*, *Mmp-9*, and *-13* transcripts. The difference between juvenile and middle-aged animals was more obvious than that between the middle-aged and elderly. Although no difference of the length density and surface density of blood vessels was detected between the middle-aged and elderly at 7 days after fracture, *Mmp-9* and *-13* were differentially expressed in these two adult age groups at a later time point (21 days after fracture, Fig. 5K, L and Fig. 6K, L). These data indicate that the angiogenic response during fracture healing is more robust in the juvenile animals than in the adults and that elderly animals may have decreased angiogenic response compared to middle-aged animals.

Age affects the expression of HIF-1 α and VEGF in fracture calluses

In our current work, we observed that the age-related decreases in endothelial surface area were directly correlated with decreased expression of factors that regulate the process of angiogenesis. HIF-1 is an oxygen tension-dependent transcription factor. This molecule is a dimer composed of an alpha subunit and a beta subunit. The beta subunit is constitutively expressed, and its activity is not affected by tissue oxygen tension. In contrast, the stability of the alpha subunit (HIF-1 α) is highly dependent on oxygen. HIF-1 α is rapidly degraded by prolyl hydroxylase under normoxic conditions and it is stabilized in hypoxic environments^{29, 30} or in the presence of elevated lactate³¹. HIF-1 plays critical roles in angiogenesis, erythropoiesis, cell death/survival, and glucose metabolism by regulating the expression of oxygen-related genes³², such as *VEGF*³³ and erythropoietin (a hormone that induces red blood cell formation)³⁰. There is evidence that illustrates HIF-1 and *VEGF* are important for endochondral ossification during development and adult bone repair. During embryonic bone development,

HIF-1 is expressed by chondrocytes in the developing growth plate, and a null mutation in the HIF-1 α gene leads to cell death of chondrocytes located in the center of the proliferative and hypertrophic zones of the growth plate 16. In rat femur fractures, HIF-1 α protein was detected in proliferating chondrocytes and osteoblasts in the newly formed callus 34. Interestingly, mice that are heterozygous for a null mutation in HIF-1 α have stronger fracture calluses associated with decreased apoptosis, possibly due to protracted endochondral ossification and callus remodeling 35. Similarly, VEGF is expressed by hypertrophic chondrocytes in fracture calluses 19, and this expression is regulated directly by Hif-1 35. During endochondral ossification, VEGF is an important factor that regulates the induction of vascular invasion of the hypertrophic cartilage 19. VEGF protein has been used to enhance angiogenesis and stimulate bone repair 36, 37.

In our study, HIF-1 α protein and *VEGF* transcripts were observed in fracture calluses in all three age groups, but the juvenile animals exhibited earlier expression. Both HIF-1 α and *VEGF* were predominantly expressed by chondrocytes in fracture calluses, suggesting that delayed HIF-1 α expression could impair *VEGF* expression in the adults. In addition to the delays in expression, the level of *VEGF* expression and the activity of HIF-1 α could be lower in the elderly animals compared to the young animals 38–40. These perturbations likely resulted in the delayed angiogenic response that we observed.

Age affects MMP expression during fracture healing

MMPs are a family of proteases that cleave components of the extracellular matrix (ECM), a process required for angiogenesis to proceed. Both MMP-9 and MMP-13 regulate endochondral ossification during bone development and bone regeneration. Lack of MMP-9 impairs the vascularization of hypertrophic cartilage during development and repair of bones, and this leads to delayed endochondral ossification 19, 20. Similarly, MMP-13 deficiency results in delayed resorption of hypertrophic cartilage of growth plate and also affects the remodeling of newly formed trabecular bone during bone development 21. In MMP-13 deficient mice, repair of bone injury is delayed due to retarded cartilage resorption 41. In this study, we detected delayed expression of *Mmp-9* and *Mmp-13* in the middle-aged and elderly mice. At 7 days post-fracture, the expression of *Mmp-9* and *Mmp-13* was robust in juvenile mice but not in the middle-aged and elderly. At 21 days post-fracture, the elderly mice retained high *Mmp-9* and *Mmp-13* mRNA levels while the expression of these molecules in middle-aged and juvenile was weak.

Relationship between the rate of vascularization and fracture healing

Although we demonstrated that age affects vascularization during fracture repair, the extent to which decreased vascularization in the adult animals slows fracture healing is not known. Fracture healing is a complex event that involves multiple processes, such as inflammation, vascularization, chondrogenesis, osteogenesis, and remodeling. These processes are highly dependent on, and interact with, one another. In this study, we observed that callus vascularization and the expression patterns of several angiogenesis-related molecules are impaired in adult mice compared to the juveniles. Decreased functional capacity of the vascular system is likely to decrease the amount of oxygen present at the fracture site, impair the exchange of other nutrients, and potentially lead to problems during recruitment of cells to the site of injury. These outcomes, alone or in combination, may contribute to the delays in fracture healing that we observed in the middle-aged and elderly animals when compared to juveniles⁵.

On the other hand, the molecules examined in this study were either expressed by chondrocytes or cells that degrade the cartilage matrix, and the altered expression of these molecules in adult mice appears to be highly correlated with the delayed cartilage formation and resorption,

suggesting that these age-related defects in vascularization could result from an age-dependent delay of chondrogenesis and endochondral ossification. Further work will be required to determine the causal relationship between decreased angiogenesis and delayed fracture healing in elderly animals. Nonetheless, our data provide evidence that the angiogenic potential during fracture healing changes throughout the lifespan of an animal. Based on our observations, examining the causal relationship between increased angiogenesis and accelerated fracture healing in juvenile animals could prove to be a fruitful avenue of experimentation to develop novel therapies for treating fractures in older patients.

Acknowledgments

This work is supported by grants from NIH-NIAMS (R01-AR053645-01 to T.M.), OTA (R.M. and C.L.), and Zimmer, Inc. (R.M.).

References

1. Skak SV, Jensen TT. Femoral shaft fracture in 265 children. Log-normal correlation with age of speed of healing. *Acta Orthop Scand* 1988;59:704–707. [PubMed: 3213461]
2. Desai BJ, Meyer MH, Porter S, et al. The effect of age on gene expression in adult and juvenile rats following femoral fracture. *J Orthop Trauma* 2003;17:689–698. [PubMed: 14600568]
3. Nilsson BE, Edwards P. Age and fracture healing: a statistical analysis of 418 cases of tibial. *Geriatrics* 1969;24:112–117. [PubMed: 5762691]
4. Sarmiento A, Sharpe FE, Ebramzadeh E, et al. Factors influencing the outcome of closed tibial fractures treated with functional bracing. *Clin Orthop* 1995;315:8–24. [PubMed: 7634690]
5. Lu C, Miclau T, Hu D, et al. Cellular basis for age-related changes in fracture repair. *J Orthop Res* 2005;23:1300–1307. [PubMed: 15936915]
6. Zheng H, Martin JA, Duwayri Y, et al. Impact of aging on rat bone marrow-derived stem cell chondrogenesis. *J Gerontol A Biol Sci Med Sci* 2007;62:136–148. [PubMed: 17339639]
7. Nishida S, Endo N, Yamagiwa H, et al. Number of osteoprogenitor cells in human bone marrow markedly decreases after skeletal maturation. *J Bone Miner Metab* 1999;17:171–177. [PubMed: 10757676]
8. Fan W, Crawford R, Xiao Y. Structural and cellular differences between metaphyseal and diaphyseal periosteum in different aged rats. *Bone*. 2007 Epub.
9. O'Driscoll SW, Saris DB, Ito Y, Fitzsimmons JS. The chondrogenic potential of periosteum decreases with age. *J Orthop Res* 2001;19:95–103. [PubMed: 11332626]
10. Meyer MH, Meyer RA Jr. Altered expression of mitochondrial genes in response to fracture in old rats. *Acta Orthop* 2006;77:944–951. [PubMed: 17260206]
11. Meyer RA Jr, Desai BR, Heiner DE, et al. Young, adult, and old rats have similar changes in mRNA expression of many skeletal genes after fracture despite delayed healing with age. *J Orthop Res* 2006;24:1933–1944. [PubMed: 16894589]
12. Colnot C, Lu C, Hu D, Helms JA. Distinguishing the contributions of the perichondrium, cartilage, and vascular endothelium to skeletal development. *Dev Biol* 2004;269:55–69. [PubMed: 15081357]
13. Hausman MR, Schaffler MB, Majeska RJ. Prevention of fracture healing in rats by an inhibitor of angiogenesis. *Bone* 2001;29:560–564. [PubMed: 11728927]
14. Asahara T, Kawamoto A. Endothelial progenitor cells for postnatal vasculogenesis. *Am J Physiol Cell Physiol* 2004;287:C572–C579. [PubMed: 15308462]
15. Hunt TK, Aslam RS, Beckert S, et al. Aerobically derived lactate stimulates revascularization and tissue repair via redox mechanisms. *Antioxid Redox Signal* 2007;9:1115–1124. [PubMed: 17567242]
16. Schipani E, Ryan HE, Didrickson S, et al. Hypoxia in cartilage: HIF-1 α is essential for chondrocyte growth arrest and survival. *Genes Dev* 2001;15:2865–2876. [PubMed: 11691837]
17. Richard DE, Berra E, Pouyssegur J. Angiogenesis: how a tumor adapts to hypoxia. *Biochemical and Biophysical Research Communications* 1999;266:718–722. [PubMed: 10603309]

18. Carmeliet P. VEGF as a key mediator of angiogenesis in cancer. *Oncology* 2005;69:4–10. [PubMed: 16301830]
19. Colnot C, Thompson Z, Miclau T, et al. Altered fracture repair in the absence of MMP9. *Development* 2003;130:4123–4133. [PubMed: 12874132]
20. Vu TH, Shipley JM, Bergers G, et al. MMP-9/gelatinase B is a key regulator of growth plate angiogenesis and apoptosis of hypertrophic chondrocytes. *Cell* 1998;93:411–422. [PubMed: 9590175]
21. Stickens D, Behonick DJ, Ortega N, et al. Altered endochondral bone development in matrix metalloproteinase 13-deficient mice. *Development* 2004;131:5883–5895. [PubMed: 15539485]
22. Behonick DJ, Xing Z, Lieu S, et al. Role of Matrix Metalloproteinase 13 in Both Endochondral and Intramembranous Ossification during Skeletal Regeneration. *PLoS ONE* 2007;2:e1150. [PubMed: 17987127]
23. Kreisle RA, Stebler BA, Ershler WB. Effect of host age on tumor-associated angiogenesis in mice. *J Natl Cancer Inst* 1990;82:44–47. [PubMed: 1688382]
24. Reed MJ, Karres N, Eyman D, et al. The effects of aging on tumor growth and angiogenesis are tumor-cell dependent. *Int J Cancer* 2007;120:753–760. [PubMed: 17131319]
25. Shimada T, Takeshita Y, Murohara T, et al. Angiogenesis and vasculogenesis are impaired in the precocious-aging *klotho* mouse. *Circulation* 2004;110:1148–1155. [PubMed: 15302783]
26. Lu C, Marcucio R, Miclau T. Assessing angiogenesis during fracture healing. *Iowa Orthop J* 2006;26:17–26. [PubMed: 16789443]
27. Dockery P, Fraher J. The quantification of vascular beds: a stereological approach. *Exp Mol Pathol* 2007;82:110–120. [PubMed: 17320863]
28. Howard, CV.; Reed, MG. *Unbiased stereology: three-dimensional measurement in microscopy*. New York: Springer-Verlag New York Inc; 1998.
29. Choi KS, Bae MK, Jeong JW, et al. Hypoxia-induced angiogenesis during carcinogenesis. *J Biochem Mol Biol* 2003;36:120–127. [PubMed: 12542982]
30. Stockmann C, Fandrey J. Hypoxia-induced erythropoietin production: a paradigm for oxygen-regulated gene expression. *Clin Exp Pharmacol Physiol* 2006;33:968–979. [PubMed: 17002676]
31. Trabold O, Wagner S, Wicke C, et al. Lactate and oxygen constitute a fundamental regulatory mechanism in wound healing. *Wound Repair Regen* 2003;11:504–509. [PubMed: 14617293]
32. Lee JW, Bae SH, Jeong JW, et al. Hypoxia-inducible factor (HIF-1)alpha: its protein stability and biological functions. *Exp Mol Med* 2004;36:1–12. [PubMed: 15031665]
33. Richard DE, Berra E, Pouyssegur J. Angiogenesis: how a tumor adapts to hypoxia. *Biochem Biophys Res Commun* 1999;266:718–722. [PubMed: 10603309]
34. Komatsu DE, Hadjiargyrou M. Activation of the transcription factor HIF-1 and its target genes, VEGF, HO-1, iNOS, during fracture repair. *Bone* 2004;34:680–688. [PubMed: 15050899]
35. Komatsu DE, Bosch-Marce M, Semenza GL, Hadjiargyrou M. Enhanced bone regeneration associated with decreased apoptosis in mice with partial HIF-1alpha deficiency. *J Bone Miner Res* 2007;22:366–374. [PubMed: 17181398]
36. Eckardt H, Ding M, Lind M, et al. Recombinant human vascular endothelial growth factor enhances bone healing in an experimental nonunion model. *J Bone Joint Surg Br* 2005;87:1434–1438. [PubMed: 16189323]
37. Street J, Bao M, deGuzman L, et al. Vascular endothelial growth factor stimulates bone repair by promoting angiogenesis and bone turnover. *Proc Natl Acad Sci U S A* 2002;99:9656–9661. [PubMed: 12118119]
38. Frenkel-Denkberg G, Gershon D, Levy AP. The function of hypoxia-inducible factor 1 (HIF-1) is impaired in senescent mice. *FEBS Lett* 1999;462:341–344. [PubMed: 10622722]
39. Rivard A, Fabre JE, Silver M, et al. Age-dependent impairment of angiogenesis. *Circulation* 1999;99:111–120. [PubMed: 9884387]
40. Wagatsuma A. Effect of aging on expression of angiogenesis-related factors in mouse skeletal muscle. *Exp Gerontol* 2006;41:49–54. [PubMed: 16289925]

41. Kosaki N, Takaishi H, Kamekura S, et al. Impaired bone fracture healing in matrix metalloproteinase-13 deficient mice. *Biochem Biophys Res Commun* 2007;354:846–851. [PubMed: 17275784]

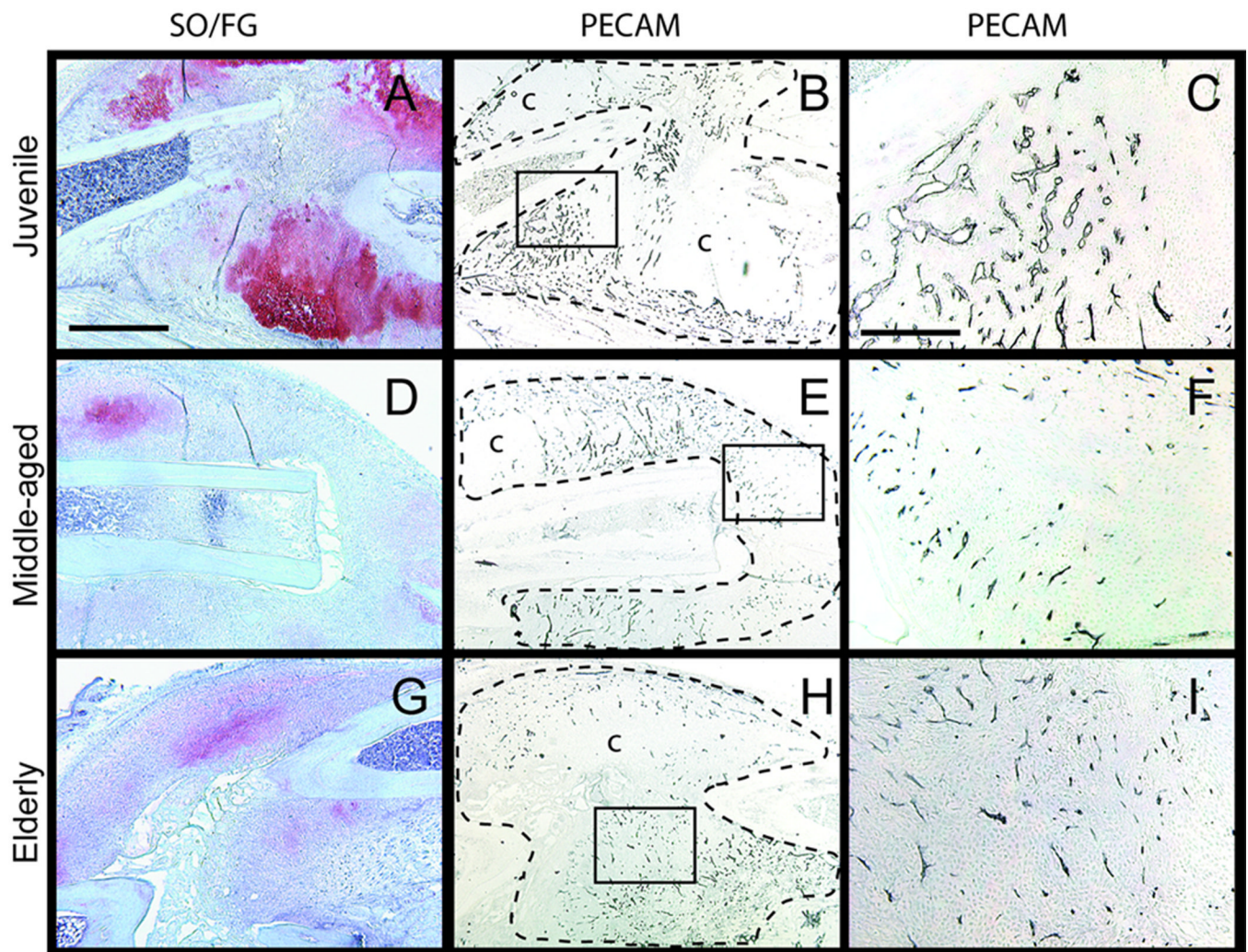


Fig. 1. Representative histograms of vascularization of fracture callus visualized by PECAM immunohistochemistry: 7 days after fracture. (A) A large amount of cartilage (red) forms in the calluses of juvenile mice. (B) Fracture calluses are well vascularized with islands of avascular cartilage (c). (C) High magnification of the box in (B) shows vascular invasion into cartilage islands. (D) A small amount of immature cartilage is present in fracture calluses of middle-aged and (G) an elderly mice. (E) Fracture calluses of (E) middle-aged and (H) elderly mice are vascularized, however, (F) blood vessels in the middle-aged and (I) elderly appear smaller than these in the juvenile. Scale bars: (A, B, D, E, G, H) = 1mm, (C, F, I) = 100 μ m. SO/FG = Safranin O/Fast Green staining. PECAM = platelet endothelial cell adhesion molecule.

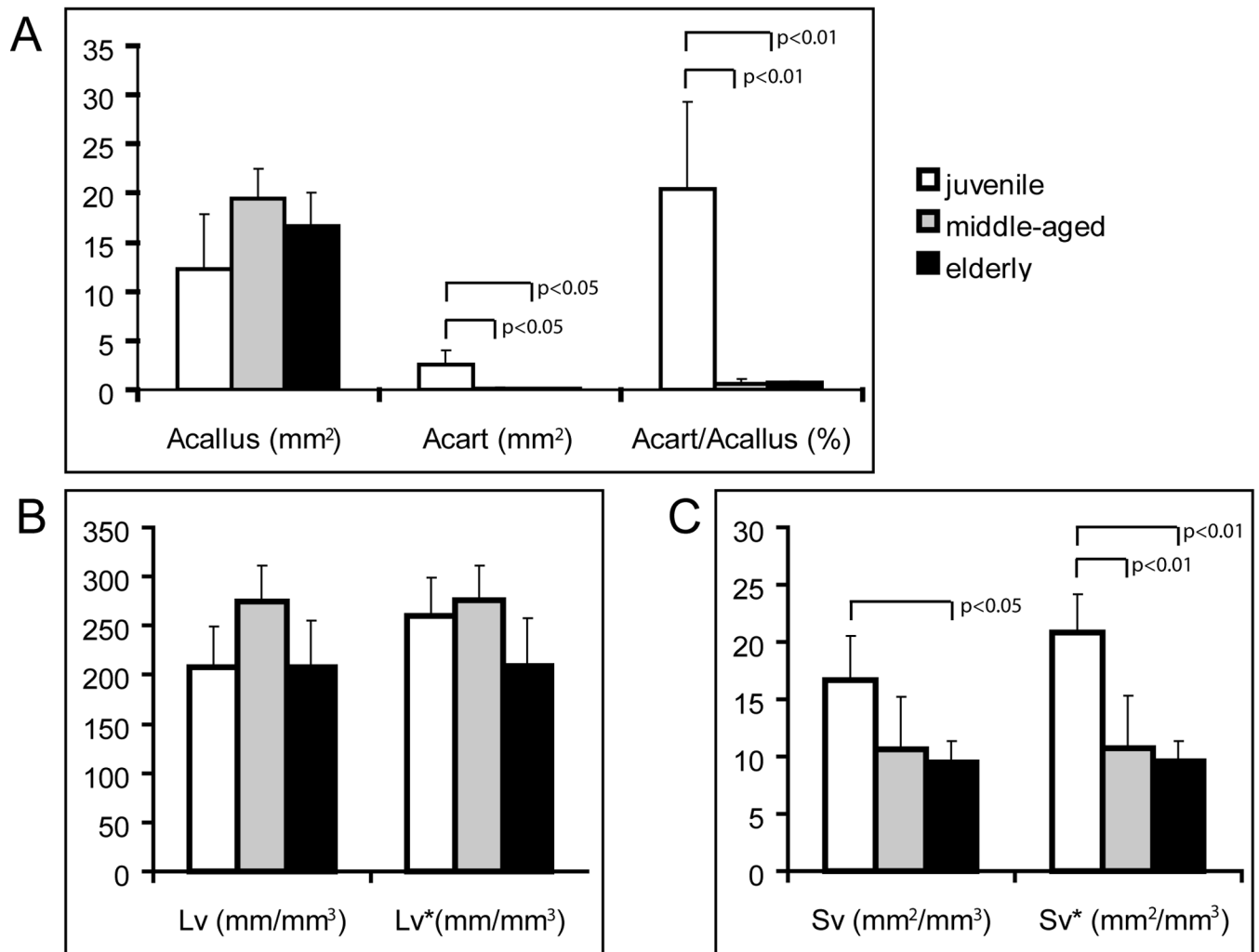


Fig. 2. Histomorphometric analyses of cartilage formation and vascularization at 7 days after fracture. (A) Animals of three age groups have similar area of callus tissue (Acallus), and juvenile mice have larger area (Acart) and higher percentage of cartilage (Acart/Acallus) within the callus than the middle-aged and elderly. (B) Length density of blood vessels in the whole callus (Lv) or in the non-cartilage callus (Lv*) is not significantly different between three ages. (C) Juvenile mice have greater surface density of blood vessels in the whole callus (Sv) than the elderly. When the area of cartilage is excluded, the juveniles exhibit higher adjusted surface density (Sv*) than both middle-aged and elderly mice.

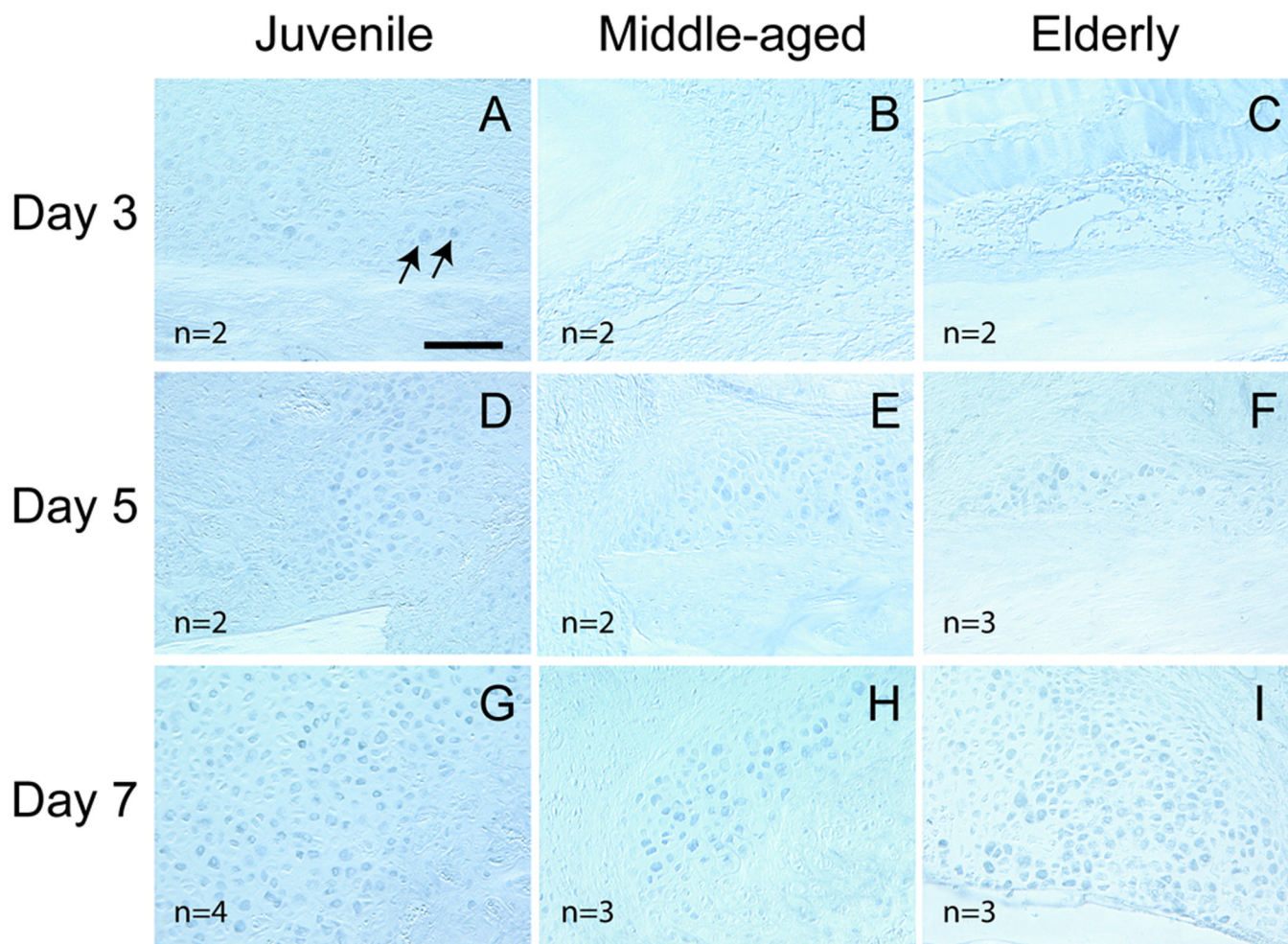


Fig. 3.

Expression of HIF-1 α detected by immunohistochemistry. (A) At 3 days post injury, a small number of chondrocytes (arrows) in the reactive periosteum of juvenile mice are positive for HIF-1 α . (B) HIF-1 α is not detected in the calluses of middle-aged and (C) elderly mice. (D–F) At 5 days, HIF-1 α is detected in the calluses of all three ages. The majority of HIF-1 α positive cells appear to be chondrocytes. (G–I) At 7 days post-fracture, HIF-1 α expression is robust in chondrocytes in all three age groups. Scale bar = 100 μ m.

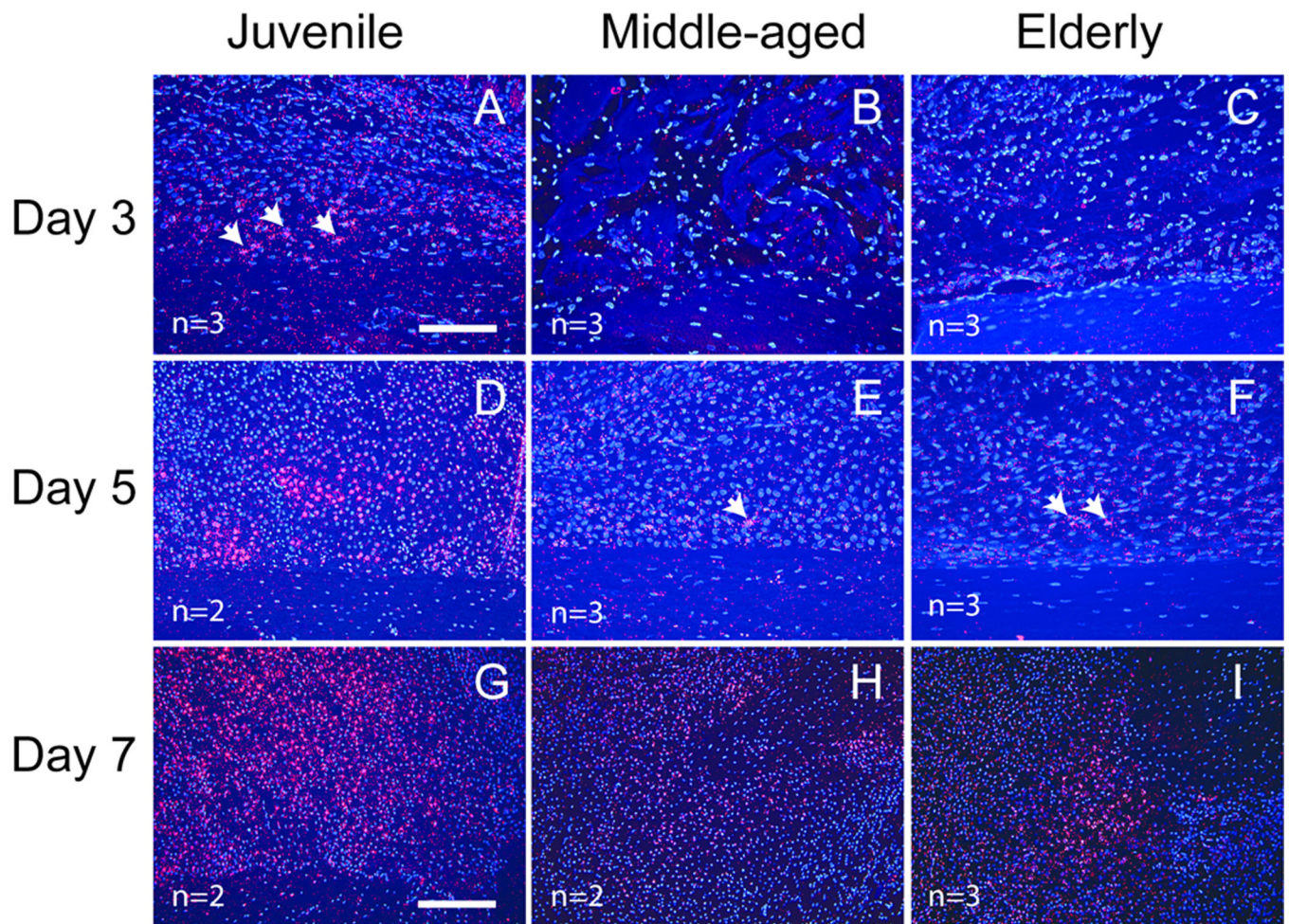


Fig. 4. Expression of *VEGF* transcript detected by *in situ* hybridization. (A) At 3 days post-injury, *VEGF* transcripts (red, arrows) are detected in chondrocytes in reactive periosteum of juvenile mice. (B) No *VEGF* expression is observed in the middle-aged and (C) elderly mice. (D) At 5 days post-fracture, *VEGF* expression is robust in the juvenile, but only a few cells (arrows) are expressing *VEGF* in (E) the middle-aged and (F) elderly. (G–I) At 7 days after fracture, *VEGF* is robustly expressed by pre-hypertrophic and hypertrophic chondrocytes in all three age groups. *VEGF* expression in the juvenile is stronger than that in the middle-aged and elderly. Scale bar: A–F = 100 μ m, G–I = 200 μ m.

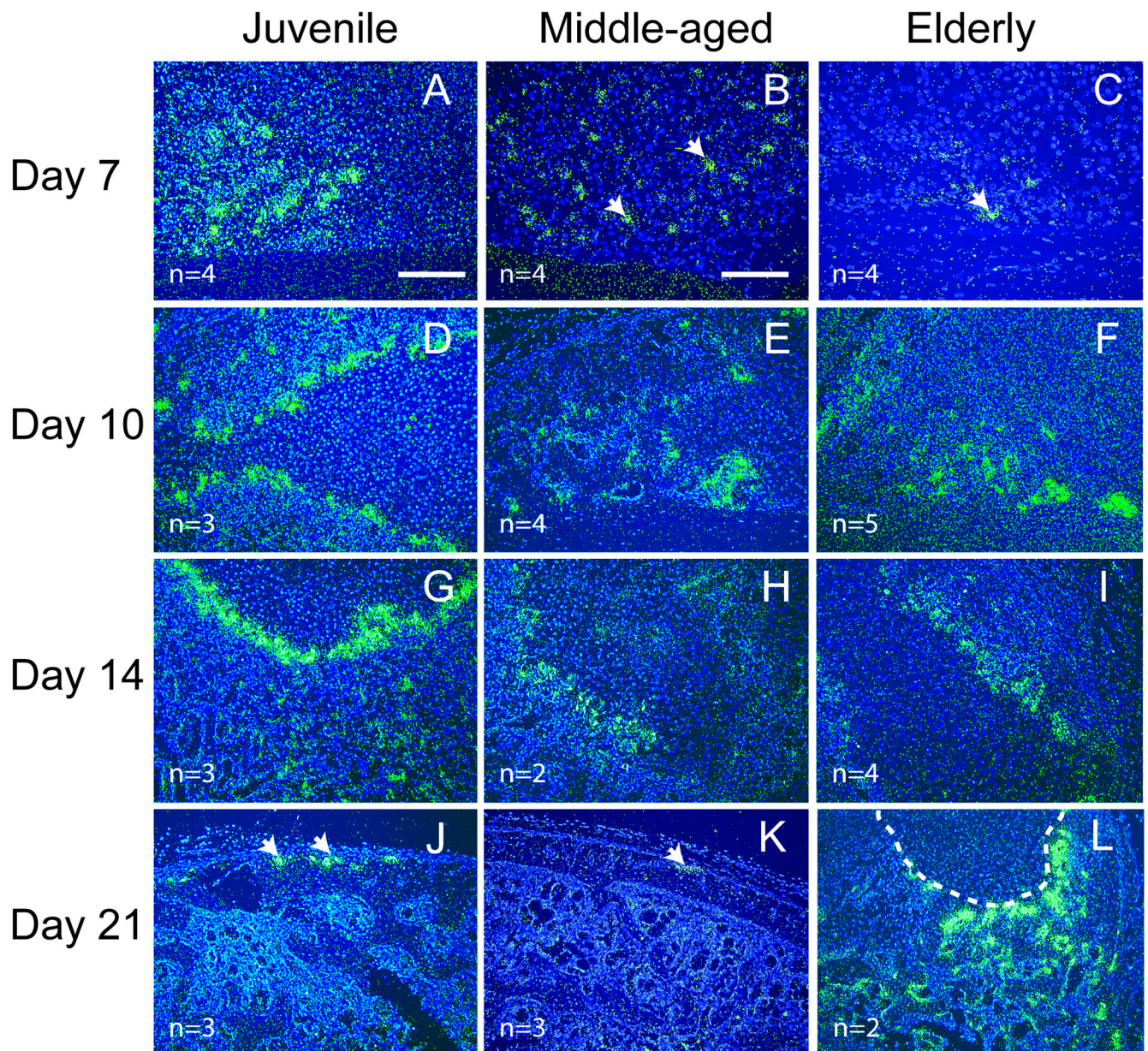


Fig. 5. Expression of *Mmp-9* detected by *in situ* hybridization. (A) At 7 days after fracture, robust *Mmp-9* expression (green) is evident at the front of endochondral ossification in juvenile mice. (B) Weak *Mmp-9* expression (arrows) is observed in middle-aged and (C) elderly mice. (D–F) At 10 days and (G–I) 14 days after fracture, strong *Mmp-9* expression is present in fracture calluses of all three age groups. (J) By 21 days, *Mmp-9* expression (arrows) is limited to the periosteum in juvenile and (K) middle-aged mice, (L) but a large amount of cartilage (outlined) and *Mmp-9* expression is still present within the calluses of the elderly. Scale bar: A, D–L = 200 μ m, B and C = 100 μ m.

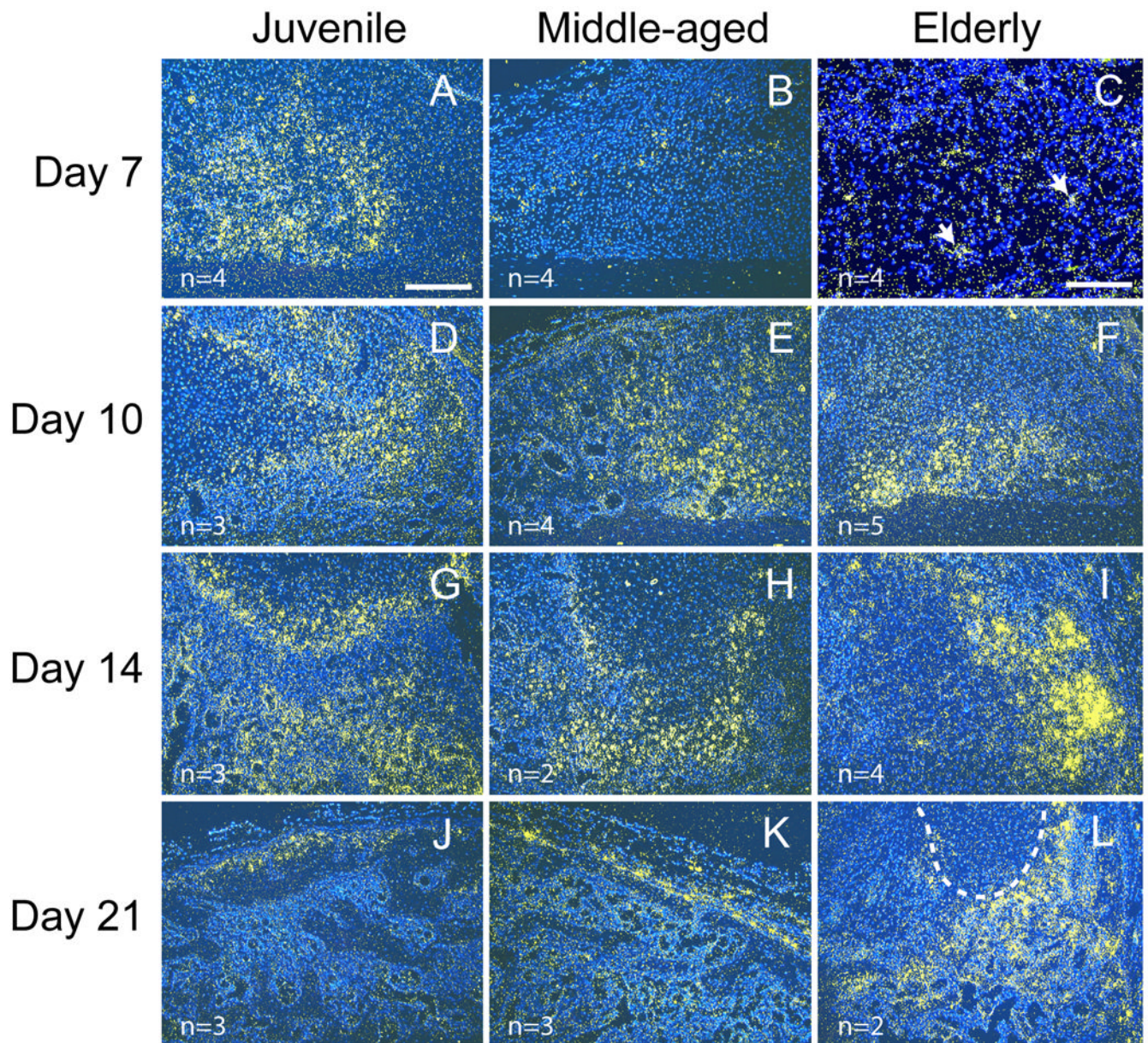


Fig. 6. Expression of *Mmp-13* detected by *in situ* hybridization. (A) At 7 days after fracture, *Mmp-13* (yellow) is strongly expressed in juvenile mice, (B) and its expression is weak in the middle-aged. (C) Just a few positive cells (arrows) are detected within fracture callus of the elderly. (D–F) Robust *Mmp-13* expression is evident in fracture calluses of all three age groups at 10 days and (G–I) 14 days after fracture. (J) At 21 days, *Mmp-13* expression is evident in fracture calluses of all three age groups at 10 days and (G–I) 14 days after fracture. (J) At 21 days, *Mmp-13* expression is low in juvenile and (K) middle-aged mice, and (L) remains high within the calluses of elderly mice. Scale bar: A, B, D–L= 200 μ m, C = 100 μ m. Outlined area in (L) is cartilage.